

Improving the accuracy of geometric model to the mark out networks for high-rise buildings

G A Shekhovtsov¹, N D Zhilina¹, A S Pavlov² and O V Raskatkina¹

¹Nizhny Novgorod State University of Architecture and Civil Engineering (NNGASU) Nizhny Novgorod 603950 Russia

²All-Russian Research Institute for Nuclear Power Plants Operation (VNIIAES), Moscow 109507 Russia

E-mail: kaf_ig@nngasu.ru

Abstract. This article describes the various options for using angular and linear-angular triangulation to create the mark out networks on the floors for high-rise buildings construction. A polynomial addition of geometric data is proposed to obtain an estimate of accuracy. The method for estimating the accuracy of geometric constructions using gradients of directions, angles and distances is considered. The numerical example shows the simplicity and high efficiency of this method. The calculations were performed using spreadsheets.

1. Introduction

The program of renovation in construction provides, in particular, the construction or reconstruction of high-rise (up to 75 meters) buildings. The main bearing elements of reinforced concrete structures in-situ of high-rise buildings are columns and floors. At the same time, it is necessary to take-away the axes grid on the floors with two types of geometrical objects – direct corner triangulation and reverse corner triangulation [1].

For this purpose, certain designated targets are installed on the day surface, for example, #1, #2, #3. On the floor, points T1, T2 and so on can be marked (figure 1). Their projections during construction will be located on each floor above this. On the floor, the auxiliary basis D-E of known length is located. Using the direct angle triangulation method the coordinates of the original points 1, 2, 3 in the building coordinate system are determined. Using the reverse corner triangulation, the coordinates of the points T1, T2, and so on are determined. From the known coordinates of the points D and E, using the principle of reduction [2], the points T1 and T2 on the floor are marked.

A method for analyzing the accuracy of the set of corner triangulation using fairly complex formulae is known [3-10]. The time spent associated with the assessment of accuracy significantly exceed the amount of information received in the form of standard deviation m_x and m_y of point T1 in the building's coordinate system. In addition, in the described method, only angular measurements are provided and there is no control over the field measurements and computational operations.

We propose an abbreviated version of the above method of increasing geometric accuracy, providing for control operations. An accuracy estimate is proposed, which allows obtaining information about the errors of the position of the point being determined.

In order to reduce the field measurements it is proposed to use points T_1 and T_2 as the end points of the *D-E* basis (figure 2).



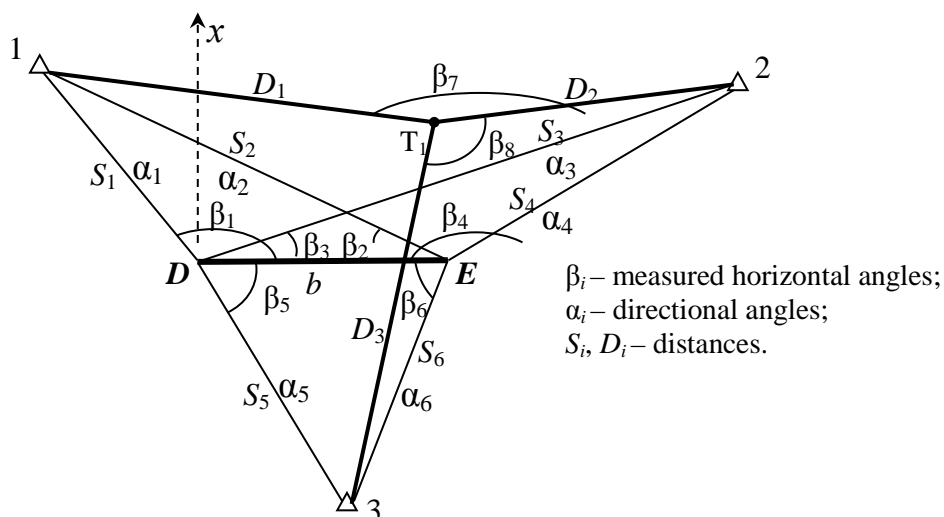


Figure 1. Determining the point T_1 on the building floor

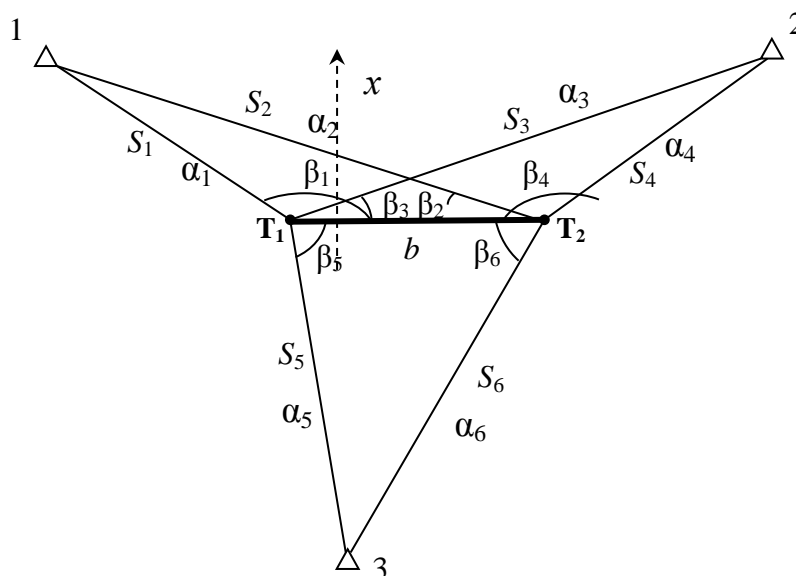


Figure 2. The abbreviated schema on the source installation horizon

2. Proposed method to improve accuracy

At the planned points T_1 and T_2 , six horizontal angles $\beta_1, \beta_2, \dots, \beta_6$ are measured. By adopting a provisory system (building coordinate system), the coordinates of target points #1, #2, #3 are calculated in this system. We note that in this case, it is not necessary to determine the coordinates of T_1 and T_2 points, which are already known, by the method of reverse angular intersection. It greatly improves the accuracy of the method.

On the upstream floor, the geometric coordinates of an auxiliary point T located approximately above the point T_1 are found using the method of reverse corner triangulation. At the same time, for the control one should measure three angles β_7, β_8 and β_9 (figure 3, b). The elements of the reduction displace the point T to the design position T_1 .

Further, by the angle β_1 and the distance b , the point T_2 can be taken out, controlling its location with the aid of the angles β_3 and β_5 . In addition, if we determine the coordinates of the remote point T_2 by the method of reverse angular triangulation, then they should be equal to 0 and b , respectively. For control, you can use the same method to determine the geometric coordinates of the outside point T_1 , which should be equal zero.

To assess the accuracy of the described method, an algorithm for constructing triangulation with angular and linear measurements is proposed.

Measured horizontal angles and distances in our case include vector values, called gradients. A visual representation of the gradients $q_{\alpha i}$ and $q_{\beta i}$ is shown in figure 3. In this figure it can be seen that for the sides with the length S_i , the direction gradients are calculated by the formula

$$q_{\alpha i} = \frac{\rho}{S_i}, \tag{1}$$

where ρ is a constant equal to 206265".

The directional angles in this case are chosen as follows: the measured angles β_2, β_4 and β_5 are right in relation to the initial side T_1-T_2 . For the measured angles, the directional angles $q_{\alpha 2}, q_{\alpha 4}$ and $q_{\alpha 5}$ will be $\alpha_{T_2-1}, \alpha_{T_2-2}$ and α_{T_1-3} . The measured angles β_1, β_3 and β_6 will be left in relation to the same side T_1-T_2 . Then the directional angles $q_{\alpha 1}, q_{\alpha 3}$ and $q_{\alpha 6}$ will be $\alpha_{1-T_1}, \alpha_{2-T_1}$ and α_{3-T_2} (figure 3, a).

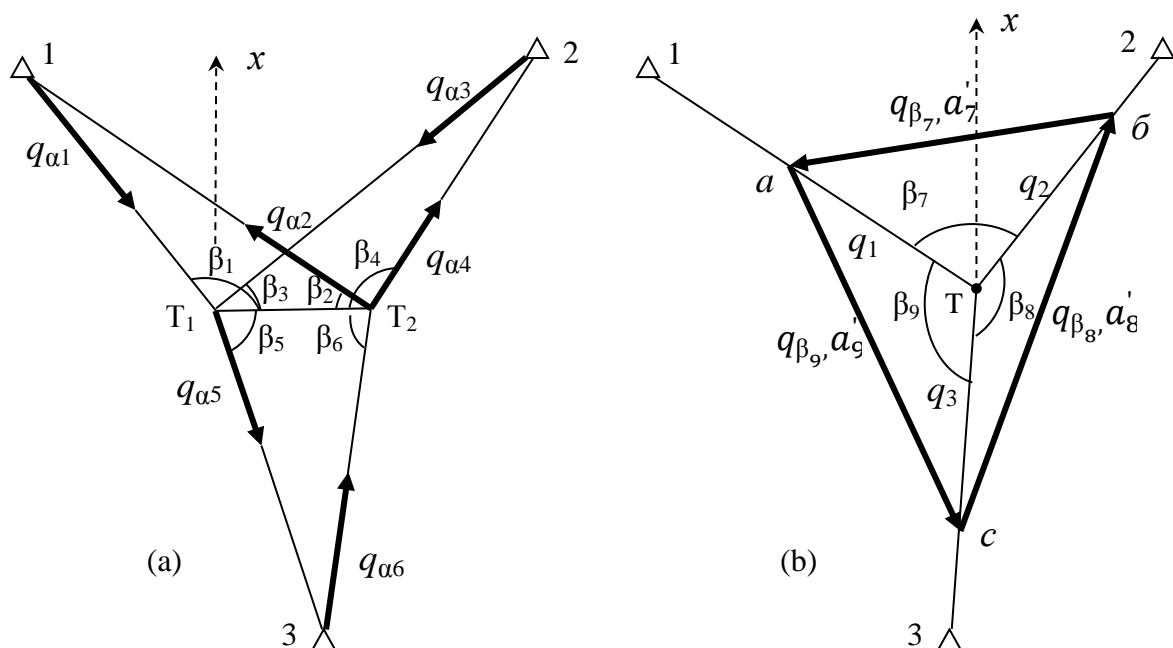


Figure 3. Gradient orientation patterns

If the angles β_7, β_8 and β_9 are measured at point T (figure 3, b), then the gradients $q_{\beta 7}, q_{\beta 8}$ and $q_{\beta 9}$ of these angles can be constructed by defining the modules of the gradients q_1, q_2, q_3 on the sides of these corners. After that, the resulting points a, b and c can be connected. The vector ab is equal to the gradient $q_{\beta 7}$, the vector bc is equal to the gradient $q_{\beta 8}$, and the vector ac is the gradient of $q_{\beta 9}$. The gradients of angles $q_{\beta i}$ are calculated by known formulae:

$$\begin{aligned} q_{\beta 7} &= \sqrt{q_1^2 + q_2^2 - 2q_1q_2\cos\beta_7} = \rho \frac{S_{1-2}}{D_1D_2}, \\ q_{\beta 8} &= \sqrt{q_2^2 + q_3^2 - 2q_2q_3\cos\beta_8} = \rho \frac{S_{2-3}}{D_2D_3}, \\ q_{\beta 9} &= \sqrt{q_1^2 + q_3^2 - 2q_1q_3\cos\beta_9} = \frac{S_{1-3}}{D_1D_3} \rho, \end{aligned} \tag{2}$$

where S_{1-2}, S_{2-3} and S_{1-3} are the distances between points 1 and 2, 2 and 3, 1 and 3, respectively, and q_1, q_2 and q_3 are gradients of the directions of the edges $1-T_1, 2-T_1$ and $3-T_1$. Gradients are calculated by equation (1).

The directions of the gradients are determined graphically or analytically. However, to calculate them by known methods, it is necessary, in addition to the distance between the source points, to know also the angles at points 1, 2, 3. Let us show by an example from [1] (figure 3, b) a simple way of

simultaneously determining the gradients $q_{\alpha i}$ and $q_{\beta i}$, based on α_i and S_i values. Initial data, triangulation and gradient calculation results are presented in table 1.

The authors have compiled a spreadsheet in which the directional angles and lengths of the triangulation are entered as source data (columns 2 and 3 of table 1).

Table 1. Reference data, gradients of directions and angles

Directions	$\alpha_i, ^\circ$	S_i, m	$q_{\alpha i},$ "/mm	q_{y_i}	q_{x_i}	Δ_{y_i}	Δ_{x_i}	$q_{\beta i}$	$\alpha'_i, ^\circ$
1	2	3	4	5	6	7	8	9	10
T-1	328	206.2	1.000	-0.5300	0.8483	0.9362	0.2097	0.96	77.4
T-2	21	182.0	1.133	0.4061	1.0580	-0.5186	-1.9736	2.04	194.7
T-3	187	223.6	0.922	-0.1124	-0.9156	-0.4177	1.7639	1.81	346.7

Gradient directions $q_{\alpha i} = \rho''/S_i$ are calculated in the table 1 (column 4). Their projections on the coordinate axis $q_{y_i} = q_{\alpha i} \cdot \sin(\alpha_i)$, $q_{x_i} = q_{\alpha i} \cdot \cos(\alpha_i)$ (columns 5 and 6), the projections on the coordinate axis of each gradient $\Delta_{y_i} = (q_{y_{(i+1)}} - q_{y_i})$, $\Delta_{x_i} = (q_{x_{(i+1)}} - q_{x_i})$ (columns 7 and 8), gradient $q_{\beta i} = \sqrt{\Delta_{y_i}^2 + \Delta_{x_i}^2}$ (column 9), their bearing $\tan^{-1}(\Delta_{y_i}/\Delta_{x_i})$ are calculated too. So we get the direction angle α'_i of gradient $q_{\beta i}$ (column 10). Similar results are obtained by graphical construction.

The values of gradients and their directional angles are used to determine the perimeter P_α and the closing line QZ of the polynomial polygon. In the case under consideration, only angular measurements of the perimeter P_α of the polygon of each right angle triangulation (figure 3, a), and perimeter P_β of reverse corner triangulation (figure 3, b) will be equal to:

$$P_\alpha = \sum q_\alpha^2, P_\beta = \sum q_\beta^2 \quad (3)$$

The line connecting the end and start points of each polygon QZ and its bearing $2\varphi'$ are determined by the formulae given in [2]:

$$(q_z)^2 = (q_y)^2 + (q_x)^2 = [q_{\alpha, \beta}^2 \sin 2\alpha]^2 + [q_{\alpha, \beta}^2 \cos 2\alpha]^2, \quad (4)$$

$$2\varphi' = \text{tg}^{-1} \frac{q_y}{q_x} = \text{tg}^{-1} \frac{[q_{\alpha, \beta}^2 \sin 2\alpha]}{[q_{\alpha, \beta}^2 \cos 2\alpha]},$$

where q_y and q_x are projections of the vector, α is the directional angle of the gradient q_α or q_β respectively.

The bearing $2\varphi'$ is determined by the signs of q_y and q_x . According to these indicators, the directional angle φ of the semi-major axis A of the error ellipse is found. The semi-major and semi-minor axes of the ellipse are based on the magnitude of the perimeter P and closing line q_3 :

$$A = m_\beta \sqrt{\frac{2}{P - q_3}}, \quad B = m_\beta \sqrt{\frac{2}{P + q_3}}, \quad (5)$$

where m_β is the standard deviation of the angles.

The accuracy of determining the position of the point T on the floor of the building by the combined method of angular triangulation depends on the accuracy of determining the coordinates of the targets 1, 2, 3 (figure 3, a), and also from precisely the opposite corner triangulation 1-2-3- T (figure 3, b). Here, the most "weak links" are three right angle triangulation 1- T_1 - T_2 , 2- T_1 - T_2 and 3- T_1 - T_2 . Their geometry has a major impact on the accuracy of determining the coordinates of targets 1, 2, 3 and on the shape and size of the error ellipse of each triangulation. The semi-major axis of the ellipse is always located inside the acute angle of the notch at points 1, 2, 3, being the most "dangerous" direction of the error of the defined point position. In order to determine the degree of

influence of right angle triangulation on the shape and size of the error ellipse, a sign simulation was performed (figure 4).

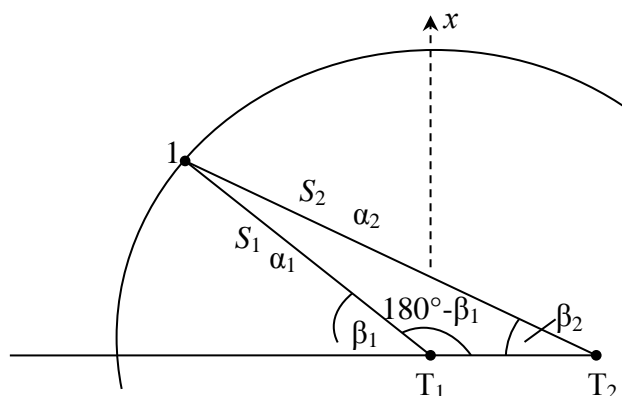


Figure 4. Simulation of straight angle triangulation

The model is a sharp triangle $I-T_1-T_2$, in which the edge T_1-T_2 was taken to be 50 m, and the directional angle is 90° . The method of modeling was that the edge of the $I-T_1$ triangle was consistently given values of 100, 200, 300 m at an angle β_1 equal to 10, 20, 40, 60, 80, 100 and 120° . The length of the other edge S_2 and the angle β_2 were calculated by the cosine theorem, and the directional angles α_1 and α_2 of the directions T_1-I and T_2-I are $270^\circ + \beta_1$ and $270^\circ + \beta_2$, respectively. The studies were limited only to the North-Western (NW) quarter of the rectangular coordinate system, since the considered forms of triangles can take place in the North-Eastern (NE), South-Eastern (SE) or South-Western (SW) quarters of this system. The source data of triangulation and the results of the error ellipses calculation are presented in table 2.

A spreadsheet was used in which directional angles and lengths of the triangulation sides were entered as input data (columns 2-5). Direction gradients were calculated using the above formulae (not shown in the table), the perimeter of the polygon (column 6), the sum of the projections of the polygon edges on the y - and x -axes (columns 7, 8), the end line of the polygon (column 9), the semi-major and semi-minor axes of the ellipse and its orientation (columns 10-12) too. From the bearing $2\phi'$ we can pass to the directional angle of the ellipse major axis (not shown in the table). All the results of the calculations are presented in the numerator of cells in table 2.

If we restrict ourselves only to angular measurements, then with standard derivation $m_\beta = 5''$ the values of the minor axis of the ellipse B of straight angular triangulation in the range of 100-300 m will be only 2-6 mm, while the values of the semi-major axis A at $S_1 = 100$ m will be 6 - 76 mm, with $S_1 = 200$ m will be 27 - 222 mm, and with $S_1 = 300$ m it will be 61 - 457 mm (see table 2).

These data suggest that it is not possible to reduce the values of the semi-major axis A by improving the geometry of the direct angle triangulation, since the lengths of the triangulation edges are several times longer than the length of the T_1-T_2 basis.

By the construction of high-rise buildings, the most effective way to improve the accuracy of triangulation is to perform linear-angle measurements using reflectorless total station theodolite.

To estimate the accuracy of such linear-angular triangulation, it is necessary to establish first the weights of linear p_s and angular p_α measurements. If we take $p_s = 1$, then $p_\alpha = \mu^2/m_{\alpha,\beta}^2$, but if we take $p_\alpha = 1$, then $p_s = \mu^2/m_s^2$, where μ is the unit weight error. In both cases, we will get the same accuracy assessment results. The edges of the polygon in this case are the values of p_s and $p_\alpha q_\alpha^2$, the orientation of which p_s is carried out at angles $(2\alpha + 180^\circ)$, and $p_\alpha q_\alpha^2$ - at angles 2α . Now the perimeter of the polygon will be equal to:

$$P = \Sigma p_s + \Sigma p_\alpha q_\alpha^2, \quad (6)$$

Table 2. Baseline and Accuracy Characteristics straight angular and linear-angular triangulation with $m\beta = 5''$, $mS = 3$ mm

Angle $\beta_1, ^\circ$	S_1, m	S_2, m	$\alpha_1, ^\circ$	$\alpha_2, ^\circ$	P, (""/mm) ²	$[q_{ai}^2 \sin 2\alpha]$	$[q_{ai}^2 \cos 2\alpha]$	$q_3,$ (""/mm) ²	A, mm	B, mm	Bearing $2\varphi', ^\circ$ and their directions
1	2	3	4	5	6	7	8	9	10	11	12
10	100	149.5	100	276.7	6.16	-1.90	-5.85	6.15	76	2	18.0 SW
					11.80	-0.29	-0.49	0.57	2.1	2	30.4 SW
	200	249.4	100	278.0	1.75	-0.55	-1.66	1.75	222	4	18.4 SW
20					7.35	-1.58	-1.11	1.93	3	2	54.9 SW
	300	349.4	100	278.6	0.82	-0.26	-0.78	0.82	457	6	18.8 SW
					6.42	2.99	3.30	4.45	5	2	42.2 NO
40	100	148.0	110	283.4	6.20	-3.61	-4.99	6.16	38	2	35.9 SW
					11.80	-1.39	0.14	1.40	2.2	1.9	84.4 NW
	200	247.6	110	286.0	1.76	-1.05	-1.40	1.75	111	4	36.8 SW
60					7.36	-1.37	-1.17	1.80	3	2	49.4 SW
	300	347.4	110	287.2	0.83	-0.50	-0.65	0.82	228	6	37.6 SW
					6.43	3.50	3.06	4.65	5	2	48.9 NO
80	100	142.0	130	296.9	6.36	-5.89	-1.98	6.22	18	2	71.4 SW
					12.00	-2.68	2.30	3.53	2.4	1.8	49.3 NW
	200	240.5	130	302.3	1.80	-1.71	-0.50	1.78	56	4	73.7 SW
100					7.40	-0.98	-1.44	1.75	3	2	34.2 SW
	300	339.8	130	304.6	0.84	-0.81	-0.21	0.84	117	5	75.3 SW
					6.44	4.23	2.18	4.76	6	2	62.7 NO
120	100	132.3	150	310.9	6.69	-6.09	1.78	6.35	12	2	73.7 NW
					12.30	-2.36	4.81	5.36	2.7	1.7	26.1 NW
	200	229.1	150	319.1	1.87	-1.72	0.65	1.84	39	4	69.4 NW
140					7.47	-0.75	-1.90	2.04	3	2	21.6 SW
	300	327.9	150	322.4	0.87	-0.79	0.34	0.86	81	5	66.9 NW
					6.47	4.34	1.02	4.46	5	2	76.7 NO
160	100	119.3	170	325.6	7.24	-4.24	5.08	6.62	9	2	39.9 NW
					12.80	-0.67	6.70	6.73	3	2	5.7 NW
	200	214.4	170	336.7	1.99	-1.04	1.64	1.94	31	4	32.4 NW
180					7.59	-0.80	-2.43	2.56	3	2	18.2 SW
	300	312.6	170	340.9	0.91	-0.43	0.79	0.90	66	5	28.7 NW
					6.51	3.73	-0.01	3.73	4	2	89.8 SO
200	100	103.7	190	341.7	8.21	-0.90	7.17	7.23	7	2	7.2 NW
					13.80	1.72	7.56	7.75	3	2	12.8 NO
	200	197.6	190	355.6	2.15	0.20	2.08	2.09	27	3	5.4 NO
220					7.75	-1.17	-2.84	3.07	3	2	22.5 SW
	300	295.4	190	0.4	0.96	0.17	0.93	0.95	61	5	10.3 NO
					6.56	2.55	-0.47	2.60	4	2	79.6 SO
240	100	86.6	210	0.0	9.93	3.68	7.80	8.63	6	2	25.3 NO
					15.50	4.64	7.63	8.93	3	1.4	31.3 NO
	200	180.3	210	16.1	2.37	1.62	1.64	2.30	27	3	44.6 NO
260					7.97	-1.67	-2.87	3.33	3	2	30.2 SW
	300	278.4	210	21.1	1.02	0.78	0.64	1.01	64	5	50.4 NO
					6.62	1.32	-0.03	1.32	3	2.5	88.6 SO

The closing line q_z and its bearing $2\varphi'$ are calculated by (4), in which its projections q_y и q_x on the axes coordinate are:

$$\begin{aligned} (q_y)^2 &= [p_\alpha q_\alpha^2 \sin 2\alpha]^2 + [p_s \sin(2\alpha + 180^\circ)]^2, \\ (q_x)^2 &= [p_\alpha q_\alpha^2 \cos 2\alpha]^2 + [p_s \cos(2\alpha + 180^\circ)]^2. \end{aligned} \quad (7)$$

The results of evaluating the accuracy of linear-angular triangulation are presented in the denominator of each cell, column 6-12 (see table 2).

The data of table 2 convincingly indicate that the most effective way to improve the accuracy of triangulation should be considered as performing linear-angle measurements. Indeed, the values of the semi-major A and semi-minor B of the ellipse in the range of 100–300 m will now be only 2–6 mm and 2– 2.5 mm, respectively. At the same time, the geometry of the triangulation has practically no effect on their accuracy.

In the proposed triangulation method, points 1, 2, 3 should be considered as starting points with respect to the point T determined by the method of reverse triangulation. Therefore, the accuracy of the position of this point should be assessed taking into account the errors of the source data. The presence of A , B and ϕ allows us to recommend for this a polynomial addition of geometric criteria that characterize the accuracy of the position of point T in a graphical or analytical way.

Consider this methodology for assessing the accuracy on the example taken from [1]. The initial data (columns 1, 2, 3, 4) and the results of estimating the accuracy of three straight lines and two reverse angular lines (figure 3) using formulae (1)...(5) with standard derivation $m_\beta = 5''$ are given in [9].

The analytical solution of the polynomial addition of geometric criteria is carried out according to the above formulae, which in this case will look like:

$$P = [(A_i^2 + B_i^2)], \tag{8}$$

$$q_3^2 = [(A_i^2 - B_i^2)\sin 2\phi_i]^2 + [(A_i^2 - B_i^2)\cos 2\phi_i]^2, \tag{9}$$

$$2\phi' = \arctg \frac{[(A_i^2 - B_i^2)\sin 2\phi_i]}{[(A_i^2 - B_i^2)\cos 2\phi_i]},$$

$$A = \sqrt{\frac{P+q_3}{2n}}, B = \sqrt{\frac{P-q_3}{2n}}. \tag{10}$$

The results of the polynomial addition of the four above-mentioned geometric criteria using the equations (8-10) are presented in table 3.

Table 3. Polynomial addition results geometric criteria for angular and linear-angular triangulation

Points	A_i , mm	B_i , mm	$2\phi_i'$, degree	q_3 , (sec/mm) ²	P, (sec/mm) ²	$2\phi_0$, degree	A_0 , mm	B_0 , mm
1	2	3	4	5	6	10	11	12
(a) Angle triangulation								
1	35.3	3.7	315					
2	35.1	3.7	2					
3	28.4	3.5	49	2641	3366	356	27.4	9.5
Reverse angle (2)	6.0	2.4	42					
Reverse angle (3)	4.41	1.88	42	2631	3347	355	27.3	9.5
(b) Linear and angle triangulation								
1	3.6	2.1	66.8					
2	3.6	2.1	115.3					
3	3.4	2.1	91.0	20.41	58.89	178.9	3.1	2.2
Reverse angle (2)	2.3	1.7	71.7					
Reverse angle (3)	1.8	1.7	54	18.58	56.84	179.5	3.1	2.2

Table 3 shows two options for reverse corner triangulation. With polynomial addition, both variants yielded almost identical results (columns 10-12). Thus, the prevailing influence on the accuracy of the position of the point T has the accuracy of determining the coordinates of the original points 1, 2, 3.

3. Conclusion

The data of table 2 and 3 convincingly indicate that the most effective way to improve the accuracy of the combined method should be the performance of linear-angular measurements.

As the examples reviewed showed, the accuracy assessment algorithm is applicable to any single or multiple triangulations. It is distinguished by simplicity, since for its implementation it is only necessary to determine the gradients of the corresponding geometric construction. The simplicity of the method makes it available even for workers who do not have special theoretical training, and the provided control operations ensure the reliability of the results obtained. It allows you to take into account all the observed linear-angular relationships of the point being defined with the reference points.

References

- [1] Klyushin E B, Zaki Mohammed Zeidan El-Sheikha and Vlasenko E P 2009 Creating horizontal range network in the assembling level when building multistorey housings *Izvestia vuzov, Geodesia I kartographia* ISSN 2618-7299 **5** 48-54 (in Russian)
- [2] Shekhovtsov G A and Ivenin D P 2017 The principle of reduction in the construction of building and structures *The Privolzhsky Scientific Journal* ISSN 1995-2511 **3** 26-34 (in Russian)
- [3] Shekhovtsov G A and Raskatkina O V 2018 About semantometric properties of the perimeter and a closure quadratic polygon an accuracy assessment cross-bearings *Geodesy and Cartography* ISSN 2587-8492 **7** 17–22 (in Russian)
- [4] Zaitsev A K, Goryainov I V and Shevchuk A A 2018 Investigation of accuracy of transmission of coordinates and heights on mounting horizons by construction of network of the resection. *Izvestia vuzov, Geodesy and Aerophotosurveying*. ISSN 2618-7299 **62 (3)** 271-276 (in Russian)
- [5] Horemuž M and Jansson P 2016 Optimum establishment of total station *Journal of Surveying Engineering* **143 (2)**.
- [6] Marshall A 2008 Analysis of free station errors *Survey Quarterly* **53** 5-7.
- [7] Pratt M J 1996 Applications of computational geometry in mechanical engineering design and manufacture In: Lin M C and Manocha D (eds) *Applied computational geometry: towards geometric engineering* **1148** 25
- [8] Kahmen H 2006 *Vermessungskunde* (Berlin: Walter de Gruyter) 679 p (in German)
- [9] Resnik B and Bill R 2018 *Vermessungskunde für den Planungs-, Bau- und Umweltbereich*. (Heidelberg: Wichmann Verlag) 380 p (in German)
- [10] Shekhovtsov G A 2018 On creation of the planned mark out network on assembling horizon while constructing the buildings of excess height *Izvestia vuzov, Geodesy and Aerophotosurveying*. ISSN 2618-7299 **62 (2)** 140-146 (in Russian)